Truncated Minimal-Norm Gauss–Newton Method Applied to the Inversion of FDEM Data

Federica Pes[0000−0001−9064−7876]

University of Pisa, 56124 Pisa, Italy federica.pes@dcci.unipi.it

Abstract. Electromagnetic induction techniques are among the most popular methods for non-invasive investigation of the soil. The collection of data is allowed by frequency domain electromagnetic devices. Starting from these data, the reconstruction of some soil properties is a challenging task, as the inverse problem is ill-posed, meaning that the problem is underdetermined, ill-conditioned, that is, the solution is sensitive to the presence of noise in the data, and nonlinear. Iterative procedures are commonly used to solve nonlinear inverse problems and the Gauss–Newton method is one of the most popular. When the problem is ill-conditioned, the Gauss–Newton method is coupled with regularization techniques, to transform the problem into a well-conditioned one. In this paper, we propose a minimal-norm regularized solution method based on the Gauss–Newton iteration to invert FDEM data. Some numerical examples on synthetic data, regarding the reconstruction of a vertical portion of the soil, show good performances.

Keywords: Inverse problems · Nonlinear least-squares · Gauss–Newton method · Regularization · FDEM.

1 Introduction

In many scientific and engineering applications, it is necessary to solve an inverse problem in order to interpret indirect physical measurements. An example of inverse problem, which will be analyzed in numerical experiments of this paper, concerns the study of the subsoil in a non-destructive way, by propagating electromagnetic waves, to obtain information about some properties. This geophysical application is described by a nonlinear model. In the following, we develop the theory for solving nonlinear least-squares problems, that can be adapted to the mentioned geophysical model. Typically, this kind of problems can be solved using iterative algorithms, such as the Gauss–Newton method. Moreover, if the problem is ill-conditioned, then it is necessary to combine the iterative method with regularization techniques to obtain an accurate solution.

The paper is organized as follows. In Section 2 we review the Gauss–Newton method and its modified version to compute the minimal-norm solution as well as some basic computational tools. Section 3 is devoted to recalling some well-known regularization techniques and to introduce the truncated MNGN2. Section 4 briefly describes a nonlinear model involved in applied geophysics and

its discretization. In Section 5 we show some numerical examples that test the different regularization techniques to reconstruct a two-dimensional vertical section of the ground and we illustrate some advantages of the TMNGN2 method. Finally, Section 6 contains concluding remarks and outlines future research.

2 Mathematical Background

We consider the nonlinear least-squares problem

$$\min_{\mathbf{x}\in\mathbb{R}^n} \|\mathbf{r}(\mathbf{x})\|_2^2, \qquad \mathbf{r}(\mathbf{x}) = F(\mathbf{x}) - \mathbf{b}, \tag{1}$$

where $F : \mathbb{R}^n \to \mathbb{R}^m$ is a nonlinear and at least twice continuously Fréchet differentiable function, $\mathbf{r}(\mathbf{x})$ represents the residual vector function between the model expectation $F(\mathbf{x})$ and the known vector $\mathbf{b} \in \mathbb{R}^m$ of measured data, and $\|\cdot\|_2$ denotes the Euclidean norm, i.e., $\|\mathbf{r}(\mathbf{x})\|_2^2 = \sum_{i=1}^m (r_i(\mathbf{x}))^2$. The problem (1) arises very frequently in data-fitting applications, in particular for parametrized physical, chemical, or financial system in which the minimum sum of squared errors measures the discrepancy between the model and the output of the system at various observation points.

Nonlinear least-squares problems can be solved using optimization approaches, as Newton's method [3,35], but more efficient and less expensive variants are often used instead. Indeed, Newton's method requires the computation of partial second derivatives of $\mathbf{r}(\mathbf{x})$ at each iteration. By ignoring the second-order term [30,37], Newton's method yields the Gauss–Newton method. If the functions $r_i(\mathbf{x})$ are mildly nonlinear in a neighborhood of the solution or if the problem is consistent (i.e., $\mathbf{r}(\mathbf{x}) = \mathbf{0}$), the behavior of the Gauss–Newton method is alike to that of Newton's method.

The *Gauss–Newton method* is based on a sequence of linear approximations of $\mathbf{r}(\mathbf{x})$, so that only first-order differential information on the model is needed. Starting with an initial guess $\mathbf{x}^{(0)}$, if $\mathbf{x}^{(k)}$ denotes the current approximation, then the new approximation is

$$\mathbf{x}^{(k+1)} = \mathbf{x}^{(k)} + \alpha_k \mathbf{s}^{(k)}, \qquad k = 0, 1, 2, \ldots, \tag{2}$$

where the step $\mathbf{s}^{(k)}$ is computed as a solution to the linear least-squares problem

$$\min_{\mathbf{s}\in\mathbb{R}^n} \|J(\mathbf{x}^{(k)})\mathbf{s} + \mathbf{r}(\mathbf{x}^{(k)})\|_2^2. \tag{3}$$

Here, $J(\mathbf{x}) \in \mathbb{R}^{m\times n}$ represents the Jacobian matrix of the function $\mathbf{r}(\mathbf{x})$,

$$[J(\mathbf{x})]_{ij} = \frac{\partial r_i(\mathbf{x})}{\partial x_j}, \qquad i = 1, \ldots, m, \quad j = 1, \ldots, n.$$

To improve convergence, we employ line search with the parameter $\alpha_k > 0$, which can be estimated by any strategy that guarantees a reduction in the norm of the residual. The choice of the step length is a trade-off between giving a substantial

reduction in the norm of the residual and, at the same time, not spending too much time finding the solution. If the scalar α_k is chosen too small, convergence is slow. We choose the step length by the *Armijo–Goldstein principle* [1,3,22]: it is determined as the largest number in the sequence $1/2^i$, $i = 0, 1, \ldots$, for which the following inequality holds

$$\|\mathbf{r}_k\|_2^2 - \|\mathbf{r}(\mathbf{x}^{(k)} + \alpha_k \mathbf{s}^{(k)})\|_2^2 \geq \frac{1}{2}\alpha_k \|J_k \mathbf{s}^{(k)}\|_2^2, \tag{4}$$

where $J_k = J(\mathbf{x}^{(k)})$ and $\mathbf{r}_k = \mathbf{r}(\mathbf{x}^{(k)})$. The solution of the least-squares problem (3) is given by

$$\mathbf{s}^{(k)} = -J_k^{\dagger} \mathbf{r}_k, \tag{5}$$

where $J_k^{\dagger}$ represents the Moore-Penrose pseudoinverse of J_k. This is a descent direction if J_k has full rank. Under this assumption, if $m \geq n$ the pseudoinverse is defined as $J_k^{\dagger} = (J_k^T J_k)^{-1} J_k^T$, otherwise, if $m < n$, it is $J_k^{\dagger} = J_k^T (J_k J_k^T)^{-1}$.

According to the definition given by Hadamard [25], problem (3) can be ill-posed, in particular, the uniqueness of the solution is not always ensured. This occurs when the system is underdetermined ($m < n$), or when the Jacobian matrix J is rank-deficient at the point $\mathbf{x}^{(k)}$.

In case of a non-unique solution, the one computed by Eq. (5) is the so-called minimal-norm solution, that is the one obtained by solving the minimal-norm linear least-squares problem

$$\min_{\mathbf{s}\in\mathbb{R}^n} \|\mathbf{s}\|_2^2, \quad \text{s.t. } \mathbf{s} \in \left\{ \arg\min_{\mathbf{s}\in\mathbb{R}^n} \|J_k \mathbf{s} + \mathbf{r}_k\|_2^2 \right\}. \tag{6}$$

To select a different solution for the step $\mathbf{s}^{(k)}$ of the new iterate $\mathbf{x}^{(k+1)}$, a matrix $L \in \mathbb{R}^{p\times n}$ ($p \leq n$) can be introduced in the objective function of problem (6), that is,

$$\min_{\mathbf{s}\in\mathbb{R}^n} \|L\mathbf{s}\|_2^2, \quad \text{s.t. } \mathbf{s} \in \left\{ \arg\min_{\mathbf{s}\in\mathbb{R}^n} \|J_k \mathbf{s} + \mathbf{r}_k\|_2^2 \right\}. \tag{7}$$

The matrix L is typically a diagonal weighting matrix or a $p \times n$ discrete approximation of a derivative operator, in which case L is a banded matrix with full row rank. For example, the matrices

$$D_1 = \begin{bmatrix} -1 & 1 & & \\ & \ddots & \ddots & \\ & & -1 & 1 \end{bmatrix} \quad \text{and} \quad D_2 = \begin{bmatrix} 1 & -2 & 1 & & \\ & \ddots & \ddots & \ddots & \\ & & 1 & -2 & 1 \end{bmatrix}, \tag{8}$$

of size $(n-1) \times n$ and $(n-2) \times n$, respectively, are approximations to the first and second derivative operators.

We remark that both problems (6) and (7) impose a regularity constraint on the update vector $\mathbf{s}$ for the solution $\mathbf{x}^{(k)}$, and not on the solution itself. The consequence of imposing a regularity constraint directly on the solution $\mathbf{x}$ of problem (1)

$$\min_{\mathbf{x}\in\mathbb{R}^n} \|L\mathbf{x}\|_2^2, \quad \text{s.t. } \mathbf{x} \in \left\{ \arg\min_{\mathbf{x}\in\mathbb{R}^n} \|F(\mathbf{x}) - \mathbf{b}\|_2^2 \right\}$$

has been analyzed in [20,37,38]. Considering an iterative method of the type (3), the step $\mathbf{s}^{(k)}$ is the solution of the linearized problem

$$\min_{\mathbf{s}\in\mathbb{R}^n} \|L(\mathbf{x}^{(k)} + \alpha\mathbf{s})\|_2^2, \quad \text{s.t. } \mathbf{s} \in \left\{\arg\min_{\mathbf{s}\in\mathbb{R}^n} \|J_k\mathbf{s} + \mathbf{r}_k\|_2^2\right\}. \tag{9}$$

In [37], the authors have shown that the iteration of the minimal-norm Gauss–Newton (MNGN) method is obtained by subtracting a projection term onto the null space of J_k to the iteration (2)

$$\mathbf{x}^{(k+1)} = \mathbf{x}^{(k)} + \alpha_k\mathbf{s}^{(k)} - \mathcal{P}_{\mathcal{N}(J_k)}\mathbf{x}^{(k)}, \qquad k = 0, 1, 2, \ldots,$$

where $\mathcal{P}_{\mathcal{N}(J_k)}$ denotes the orthogonal projector onto the null space of J_k. Then, in [38], in order to avoid some issues in the convergence caused by the projection term, the more efficient implementation (MNGN2) is proposed

$$\mathbf{x}^{(k+1)} = \mathbf{x}^{(k)} + \alpha_k\mathbf{s}^{(k)} - \beta_k\mathcal{P}_{\mathcal{N}(J_k)}\mathbf{x}^{(k)}, \qquad k = 0, 1, 2, \ldots, \tag{10}$$

where the parameter β_k controls that the projection does not cause an increase in the residual. In the same paper, some techniques to estimate it are explained in detail.

In the case of an ill-conditioned problem, it is necessary to regularize it. Classical regularization techniques are the T(G)SVD and the Tikhonov method. In this paper, we introduce the truncated MNGN2 method, that is a regularized version of the MNGN2 method (10). We stress that the MNGN2 method has been introduced in [38] for well-conditioned problems. Herein, we extend it for ill-conditioned problems. Moreover, we apply the truncated MNGN2 algorithm to an applied geophysics problem, with the aim of reconstructing a 2D section of the subsurface.

We end this section by introducing some useful tools. We recall the definition of the singular value decomposition (SVD) of a matrix J as well as that of the generalized singular value decomposition (GSVD) of a matrix pair (J, L) [24].

The SVD is a matrix decomposition of the form

$$J = U\Sigma V^T, \tag{11}$$

where the diagonal matrix $\Sigma \in \mathbb{R}^{m\times n}$ contains the *singular values* ordered such that $\sigma_1 \geq \sigma_2 \geq \cdots \geq \sigma_r > 0$, with $r = \text{rank}(J) \leq \min(m, n)$, and the matrices $U = [\mathbf{u}_1, \ldots, \mathbf{u}_m] \in \mathbb{R}^{m\times m}$ and $V = [\mathbf{v}_1, \ldots, \mathbf{v}_n] \in \mathbb{R}^{n\times n}$ have orthonormal columns.

Let $J \in \mathbb{R}^{m\times n}$ and $L \in \mathbb{R}^{p\times n}$ be matrices with $\text{rank}(J) = r$ and $\text{rank}(L) = p$. Suppose that $m + p \geq n$ and

$$\text{rank}\left(\begin{bmatrix} J \\ L \end{bmatrix}\right) = n,$$

or, equivalently, that $\mathcal{N}(J) \cap \mathcal{N}(L) = \{0\}$. The GSVD of the matrix pair (J, L) is defined by the factorizations

$$J = U\Sigma_J W^{-1}, \qquad L = V\Sigma_L W^{-1}, \tag{12}$$

where $U \in \mathbb{R}^{m\times m}$ and $V \in \mathbb{R}^{p\times p}$ are matrices with orthonormal columns $\mathbf{u}_i$ and $\mathbf{v}_i$, respectively, and $W \in \mathbb{R}^{n\times n}$ is nonsingular. If $m \geq n \geq r$, the structure of the matrices $\Sigma_J \in \mathbb{R}^{m\times n}$ and $\Sigma_L \in \mathbb{R}^{p\times n}$ is

$$\Sigma_J = \left[\begin{array}{c} O_{n-r} \\ \hline C \\ \hline \\ \hline I_d \\ \hline \\ O_{(m-n)\times n} \end{array}\right], \qquad \Sigma_L = \left[\begin{array}{c|c} I_{p-r+d} & \\ \hline & O_{p\times d} \\ \hline S & \end{array}\right],$$

where $d = n-p$, and the blocks C and S are nonnegative diagonal matrices such that

$$\begin{aligned} C &= \operatorname{diag}(c_1, \ldots, c_{r-d}), & 0 < c_1 \leq c_2 \leq \cdots \leq c_{r-d} < 1, \\ S &= \operatorname{diag}(s_1, \ldots, s_{r-d}), & 1 > s_1 \geq s_2 \geq \cdots \geq s_{r-d} > 0, \end{aligned}$$

with $c_i^2 + s_i^2 = 1$, for $i = 1, \ldots, r-d$. The identity matrix of size k is denoted by I_k, while O_k and $O_{k\times\ell}$ are zero matrices of size k and $k \times \ell$, respectively; if one of the dimensions of the identity or zero submatrices vanishes, the block has to be omitted. The *generalized singular values* are the scalars $\gamma_i = c_i/s_i$, and they appear in nondecreasing order. If $r \leq m < n$, the matrix $\Sigma_J \in \mathbb{R}^{m\times n}$ has the form

$$\Sigma_J = \left[\begin{array}{c|c} O_{m\times(n-m)} & \begin{array}{ccc} O_{m-r} & & \\ & C & \\ & & I_d \end{array} \end{array}\right],$$

where the blocks are defined as above, and the structure of $\Sigma_L \in \mathbb{R}^{p\times n}$ is the same as the previous one.

3 TGSVD, TMNGN2, and Tikhonov Regularization

In applications, typically, the measured data vector $\mathbf{b}$ is prone to noise caused by measurement errors. This results in a perturbed data vector

$$\mathbf{b} = \widehat{\mathbf{b}} + \mathbf{e}, \qquad \mathbf{e} \in \mathbb{R}^m,$$

where $\widehat{\mathbf{b}} \in \mathbb{R}^m$ is the exact data vector and $\mathbf{e} \in \mathbb{R}^m$ represents the noise vector. Due to error propagation, the computed solution may deviate significantly from the exact solution, especially in ill-conditioned problems. It is well-known that the concept of inverse problem is closely related to that of ill-conditioning. A nonlinear operator $F(\mathbf{x})$ is considered ill-conditioned in a domain $\Omega \subset \mathbb{R}^n$ when the condition number $\kappa(J)$ of the Jacobian $J = J(\mathbf{x})$ is very large for any $\mathbf{x} \in \Omega$. In such cases, a common approach is to apply a regularization procedure at each step of the Gauss–Newton method: the initial least-squares problem is replaced by a nearby better conditioned problem, whose solution is less sensitive to the error $\mathbf{e}$ in the right-hand side $\mathbf{b}$ and to round-off errors introduced during the solution process. For a more detailed discussion regarding regularization of inverse problems, we refer to [19,27].

One of the most widely used methods to do so is the truncated singular value decomposition applied to the system matrix. The TSVD solves (6) after substituting J_k by its best rank-ℓ approximation. Here, ℓ is the regularization parameter, which has to be wisely estimated. Choosing its value amounts to finding a compromise between fidelity to the original model and numerical stability.

Fixed a value for the truncation parameter $1 \leq \ell \leq r$, the iteration of the truncated Gauss–Newton method becomes

$$\mathbf{x}_\ell^{(k+1)} = \mathbf{x}_\ell^{(k)} - \alpha_k \sum_{i=1}^{\ell} \frac{\mathbf{u}_i^T \mathbf{r}(\mathbf{x}_\ell^{(k)})}{\sigma_i} \mathbf{v}_i, \qquad k = 0, 1, 2, \ldots, \tag{13}$$

where $\mathbf{u}_i$ and $\mathbf{v}_i$ are the left and right singular vectors of J_k, respectively; see Eq. (11). We remark that the singular value decomposition of the matrix J_k changes at each step of the Gauss–Newton method, and that the rank r may change too. In order not to burden the notation we write $\mathbf{u}_i$, $\mathbf{v}_i$, σ_i, and r without specifying the dependence on k.

On the other hand, if the step $\mathbf{s}^{(k)}$ is determined by regularizing problem (7), the iteration is expressed in terms of the GSVD of the matrix pair (J_k, L):

$$\mathbf{x}_\ell^{(k+1)} = \mathbf{x}_\ell^{(k)} - \alpha_k \sum_{i=p-\ell+1}^{p} \frac{\mathbf{u}_{i-N}^T \mathbf{r}(\mathbf{x}_\ell^{(k)})}{c_{i-n+r}} \mathbf{w}_i - \alpha_k \sum_{i=p+1}^{n} (\mathbf{u}_{i-N}^T \mathbf{r}(\mathbf{x}_\ell^{(k)})) \mathbf{w}_i,$$

where the integer $0 \leq \ell \leq p - n + r$ is the regularization parameter, $\mathbf{u}_{i-N}$ and $\mathbf{w}_i$ are the column vectors of the matrices U and W of (12), respectively, and the integer $N = \max(n - m, 0)$ allows us to condense in a single formula both the overdetermined and underdetermined case. As in the previous formulation, the GSVD of (J_k, L) changes at each iteration, therefore the same observation made before on the abuse of notation by not indicating the dependence on k of $\mathbf{u}_{i-N}$, $\mathbf{w}_i$, c_{i-n+r}, and r is valid.

The truncated MNGN2 method solves (9), when $L = I_n$, considering the best rank-ℓ approximation of J_k. As remarked in Section 2, the iteration of the TMNGN2 method differs from that of the truncated Gauss–Newton (13) for the presence of a projection term. Indeed it is of the form

$$\mathbf{x}_\ell^{(k+1)} = \mathbf{x}_\ell^{(k)} - \alpha_k \sum_{i=1}^{\ell} \frac{\mathbf{u}_i^T \mathbf{r}(\mathbf{x}_\ell^{(k)})}{\sigma_i} \mathbf{v}_i - \beta_k \sum_{i=\ell+1}^{n} (\mathbf{v}_i^T \mathbf{x}_\ell^{(k)}) \mathbf{v}_i, \qquad k = 0, 1, 2, \ldots.$$

Similarly, if $L \neq I_n$, the TMNGN2 iteration depends on the GSVD of (J_k, L) and it is given by

$$\begin{aligned} \mathbf{x}_\ell^{(k+1)} = \mathbf{x}_\ell^{(k)} &- \alpha_k \sum_{i=p-\ell+1}^{p} \frac{\mathbf{u}_{i-N}^T \mathbf{r}(\mathbf{x}_\ell^{(k)})}{c_{i-n+r}} \mathbf{w}_i - \alpha_k \sum_{i=p+1}^{n} (\mathbf{u}_{i-N}^T \mathbf{r}(\mathbf{x}_\ell^{(k)})) \mathbf{w}_i \\ &- \beta_k \sum_{i=1}^{p-\ell} (\widehat{\mathbf{w}}^i \mathbf{x}_\ell^{(k)}) \mathbf{w}_i, \end{aligned}$$

where $\widehat{\mathbf{w}}^i$ are the row vectors of the matrix W^{-1}; see Eq. (12). The non-regularized version of the last two formulas has been obtained in [38].

Another approach consists of regularizing the least-squares problem (3) by the Tikhonov method, that is, solving the minimization problem

$$\min_{\mathbf{s}\in\mathbb{R}^n} \left\{ \|J_k\mathbf{s} + \mathbf{r}_k\|_2^2 + \lambda^2 \|L\mathbf{s}\|_2^2 \right\}, \tag{14}$$

for a fixed value of the parameter $\lambda > 0$ and a chosen regularization matrix $L \in \mathbb{R}^{p\times n}$. The regularization parameter λ controls the balance between the two terms of the functional, i.e., the weights attributed to the residual term and to the regularization term. Equivalently, (14) can be written as

$$\min_{\mathbf{s}\in\mathbb{R}^n} \left\| \begin{bmatrix} J_k \\ \lambda L \end{bmatrix} \mathbf{s} + \begin{bmatrix} \mathbf{r}_k \\ \mathbf{0} \end{bmatrix} \right\|_2^2.$$

The solution of (14) is given by

$$\mathbf{s} = -(J_k^T J_k + \lambda^2 L^T L)^{-1} J_k^T \mathbf{r}_k.$$

Then, if $L = I_n$, after substituting the SVD of J_k, the iteration of the Gauss–Newton method with Tikhonov regularization is

$$\mathbf{x}_\lambda^{(k+1)} = \mathbf{x}_\lambda^{(k)} - \alpha_k \sum_{i=1}^{r} \frac{\sigma_i(\mathbf{u}_i^T \mathbf{r}(\mathbf{x}_\lambda^{(k)}))}{\sigma_i^2 + \lambda^2} \mathbf{v}_i, \qquad k = 0, 1, 2, \ldots,$$

where $\{\mathbf{u}_i, \mathbf{v}_i, \sigma_i\}$ are the singular triplets of J_k (Eq. (11)). If $L \neq I_n$, considering the GSVD of the matrix pair (J_k, L), the iterative method becomes

$$\mathbf{x}_\lambda^{(k+1)} = \mathbf{x}_\lambda^{(k)} - \alpha_k \sum_{i=n-r+1}^{p} \frac{c_{i-n+r}(\mathbf{u}_{i-N}^T \mathbf{r}(\mathbf{x}_\lambda^{(k)}))}{c_{i-n+r}^2 + \lambda^2 s_{i-n+r}^2} \mathbf{w}_i - \alpha_k \sum_{i=p+1}^{n} (\mathbf{u}_{i-N}^T \mathbf{r}(\mathbf{x}_\lambda^{(k)}))\mathbf{w}_i,$$

where $\mathbf{u}_{i-N}$ and $\mathbf{w}_i$ are the column vectors of the matrices U and W of (12), respectively, and $N = \max(n - m, 0)$.

3.1 Regularization Parameter Estimation

The solution vectors obtained through the Gauss–Newton method, regularized by TGSVD/TMNGN2 or by the Tikhonov approach, will be denoted by $\mathbf{x}_\ell$ or $\mathbf{x}_\lambda$ at convergence, respectively, where ℓ and λ are the corresponding regularization parameters. A regularization method should also incorporate a technique for estimating the optimal regularization parameter.

Most of the methods for determining the regularization parameter are based on residual norms and, in the case of the L-curve, also on the (semi)norm of the solution. Assuming the knowledge of the error norm $\|\mathbf{e}\|_2$ or of a good estimate of it, the discrepancy principle introduced by Morozov [34] can be used to determine the parameter. In real situations, when the noise is unknown,

heuristic techniques, as the L-curve criterion [26,28,29] or the generalized cross-validation [8,21,23], allow to estimate the regularization parameter without information on the noise level. There are many contributions dedicated to developing and analyzing different methods to select the regularization parameter. In this regard, the interested reader can see [7,27,32,36,39] and references therein.

In the numerical experiments reported in this paper, we determine the regularization parameters by the L-curve criterion. In the upcoming subsection we remind what it consists of.

L-curve. This method is based on a plot of the logarithm of the (semi)norm $\|L\mathbf{s}_{\text{reg}}\|_2$ of the regularized solution versus the logarithm of the corresponding residual norm $\|J_k\mathbf{s}_{\text{reg}} + \mathbf{r}_k\|_2$. With the subscript "reg" we refer in general to both parameters ℓ and λ, depending on the approach adopted to regularize. The L-curve is also a powerful graphical tool for the analysis of discrete ill-posed problems, since it graphically represents the compromise between the minimization of these two quantities, which is the core of any regularization method.

When the regularization parameter is continuous, as in Tikhonov regularization, the L-curve is a continuous curve. In case of regularization methods with a discrete regularization parameter, such as TGSVD/TMNGN2, the L-curve consists of a finite set of points

$$\begin{aligned}
&\Big(\log\|J_k\mathbf{s}_{\text{reg}} + \mathbf{r}_k\|_2,\ \log\|L\mathbf{s}_{\text{reg}}\|_2\Big), && \text{in TGSVD,}\\
&\Big(\log\|J_k\mathbf{s}_{\text{reg}} + \mathbf{r}_k\|_2,\ \log\|L(\mathbf{x}^{(k)} + \alpha\mathbf{s}_{\text{reg}})\|_2\Big), && \text{in TMNGN2.}
\end{aligned}$$

This criterion chooses the regularization parameter corresponding to the point of maximum curvature on the log-log plot of the L-curve, which corresponds to the corner of the "L"-shape.

4 A Nonlinear Model for FDEM Data Inversion

In this section, we briefly describe a nonlinear model typical of applied geophysics. It is based on electromagnetic induction techniques that allow to investigate in a non-destructive way some soil properties. Mathematically, it is represented by a system of first kind integral equations.

Before describing the nonlinear model, we recall that, in 1980, a linear model was developed by McNeill [33] to reproduce the readings of one of the first available ground conductivity meters (GCM), the Geonics EM-38. Regarding this model and the possibility of recovering the distribution of the electrical conductivity, in [5], a Tikhonov regularization technique was implemented to reconstruct the conductivity profile from measurements obtained by positioning a GCM at various heights above the ground, while in [9] the Tikhonov approach was optimized by a projected conjugate gradient algorithm.

More recently, in [15], the linear system has been studied under the hypothesis that the values of the unknown function are known at the boundaries. The

aforementioned paper led to propose subsequently a numerical method to compute the solution of a system of first kind integral equations in the presence of boundary constraints. The algorithm descends from the Riesz representation theorem and the solution is sought in a reproducing kernel Hilbert space. A first version of the algorithm is introduced in [16], that addresses the idea for a single integral equation. Afterwards, in [17] the theory is generalized for a system of integral equations of the first kind.

In 1982, Wait [40] described a nonlinear forward model for predicting the electromagnetic response of the subsoil. In [31], the technique adopted in [5] was extended and applied to a nonlinear model for the same physical system, previously described in [41]. A regularized inversion algorithm was studied in [12,14] and then it was extended to process complex-valued datasets [13]. The algorithm was coded in Matlab and included in the publicly available software package FDEMtools [10] which includes a graphical user interface (GUI), that has already been employed in real-world applications [4,13,18]. In [6] the authors propose to solve a variational problem to obtain a 2D reconstruction of some properties of a soil vertical section. Recently, the FDEMtools package has been updated by inserting some variants for the computation of the minimal-norm solution regarding the resolution of the inverse problem, as well as a GUI for a forward modelling [11].

In the model, the soil is assumed to have a layered structure with n layers below ground level, starting from $z_1 = 0$. Each subsoil layer, of thickness d_k (meters), ranges from depth z_k to z_{k+1}, $k = 1, \ldots, n-1$, and is characterized by an electrical conductivity σ_k (Siemens/meter) and a magnetic permeability μ_k (Henry/meter), for $k = 1, \ldots, n$. The thickness of the deepest layer d_n, starting at z_n, is considered infinite.

A GCM is an FDEM induction device composed of two coils, namely a transmitter and a receiver, positioned at a fixed distance ρ from each other. The two coils, operating at frequency f in Hertz, are at height h above the ground with their axes oriented either vertically or horizontally with respect to the ground surface. Both the depth z and the height h are measured in meters. The transmitting coil generates a primary electromagnetic (EM) field H_P above the ground, which then propagates into it. H_P induces eddy currents in the conductive parts of the subsurface, generating in succession a secondary EM field H_S, that propagates towards the ground surface. This signal is detected by the receiver. The GCM measures the ratio between the secondary EM field produced by such currents and the primary field. The reader interested on the working principles of the instrument is referred to [11] for a detailed discussion.

Mathematically, the nonlinear model, derived from Maxwell's equations, consists of two integral equations of the first kind. Let $u_k(\lambda) = \sqrt{\lambda^2 + \mathrm{i}\sigma_k\mu_k\omega}$, where i is the unit imaginary number and $\omega = 2\pi f$ is the angular frequency of the electromagnetic wave generated by the device. The variable λ is non-negative and it measures the ratio between the depth below the ground surface and the inter-coil

distance ρ. If we denote the characteristic admittance in the kth layer by

$$N_k(\lambda) = \frac{u_k(\lambda)}{\mathrm{i}\mu_k\omega}, \quad k = 1, \ldots, n,$$

then the surface admittance $Y_k(\lambda)$ at the top of the same layer verifies the recursion

$$\begin{cases} Y_n(\lambda) = N_n(\lambda), \\ Y_k(\lambda) = N_k(\lambda)\dfrac{Y_{k+1}(\lambda) + N_k(\lambda)\tanh(d_k u_k(\lambda))}{N_k(\lambda) + Y_{k+1}(\lambda)\tanh(d_k u_k(\lambda))}, \quad k = n-1, \ldots, 1. \end{cases} \tag{15}$$

as shown in [40]. Let us define the reflection factor as

$$R_\omega(\lambda) = \frac{N_0(\lambda) - Y_1(\lambda)}{N_0(\lambda) + Y_1(\lambda)},$$

where $Y_1(\lambda)$ is computed by the recursion formula (15) and $N_0(\lambda) = \lambda/(\mathrm{i}\mu_0\omega)$, with $\mu_0 = 4\pi 10^{-7}\mathrm{H/m}$ the value of the vacuum magnetic permeability, that is the permeability of the free space. The ratio of the secondary field to the primary one is given by the following system of two integral equations of the first kind

$$M_\nu(\boldsymbol{\sigma}, \boldsymbol{\mu}; h, \omega, \rho) = -\rho^{3-\nu} \int_0^\infty \lambda^{2-\nu} e^{-2h\lambda} R_\omega(\lambda) J_\nu(\rho\lambda)\, d\lambda, \qquad \nu = 0, 1,$$

by setting $\nu = 0$ and $\nu = 1$ for the vertical and horizontal orientation of the coils, respectively. In the above equation, $\boldsymbol{\sigma} = [\sigma_1, \ldots, \sigma_n]^T$, $\boldsymbol{\mu} = [\mu_1, \ldots, \mu_n]^T$, and J_ν denotes the first kind Bessel function of order ν.

As is usual in many applications, we let the magnetic permeability take the constant value μ_0 in all layers. It is reasonable to make this assumption if the ground does not contain ferromagnetic materials. Recent FDEM devices can record multiple measurements with different operating frequencies $\omega_1, \ldots, \omega_{m_\omega}$ or different inter-coil distances $\rho_1, \ldots, \rho_{m_\rho}$ at different heights $h_1, \ldots, h_{m_h}$ above the ground. Considering also both orientations of the coils, we have $m = 2m_\rho m_\omega m_h$ measurements. We denote them by $\mathbf{b} = [b_1, \ldots, b_m]^T$, and the model prediction by $M(\boldsymbol{\sigma})$, where

$$M(\boldsymbol{\sigma}) = \begin{bmatrix} M_0(\boldsymbol{\sigma}) \\ M_1(\boldsymbol{\sigma}) \end{bmatrix}.$$

Then, the problem of data inversion consists of computing the conductivity vector $\boldsymbol{\sigma}$ which determines the best fit to the data vector $\mathbf{b}$, that is, the one which solves the problem

$$\min_{\boldsymbol{\sigma} \in \mathbb{R}^n} \|\mathbf{r}(\boldsymbol{\sigma})\|_2^2, \qquad \text{with } \mathbf{r}(\boldsymbol{\sigma}) = M(\boldsymbol{\sigma}) - \mathbf{b}.$$

This is the one-dimensional discretization of the problem, i.e., considering the measurements collected by the instrument at a fixed point above the ground.

We now consider a 2D discretization of the problem. In practice, by moving the device along a straight path above the ground, it is possible to collect data

at several points. We depict the two-dimensional vertical section of the ground as the rectangle $[0, a] \times [0, b]$, where $[0, a]$ represents the horizontal path along which the instrument is moved, and $[0, b]$ is the depth under the ground; see Fig. 1. Our intention is to reconstruct the electrical conductivity as an image.

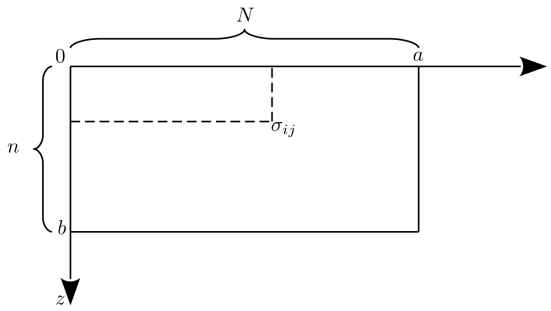

Fig. 1. 2D scheme of a vertical portion of the subsoil. The electrical conductivity of the ith layer in the jth dataset is denoted by σ_{ij}.

Given the two-dimensional section of the ground and assuming to have N equispaced measurement sets, let σ_{ij} be the electrical conductivity of the ith layer in the jth dataset, and $\boldsymbol{\sigma}_j = [\sigma_{1j}, \ldots, \sigma_{nj}]^T$, $j = 1, \ldots, N$. Let the corresponding dataset be $\mathbf{b}_j = [b_{1j}, \ldots, b_{mj}]^T$. We group them in the matrices

$$\mathbf{S} = (\sigma_{ij}) = [\boldsymbol{\sigma}_1, \ldots, \boldsymbol{\sigma}_N] \in \mathbb{R}^{n \times N}, \qquad \mathbf{B} = (b_{pj}) = [\mathbf{b}_1, \ldots, \mathbf{b}_N] \in \mathbb{C}^{m \times N}.$$

We want to solve the nonlinear least-squares problem

$$\min_{\mathbf{S}} \|\mathbf{M}(\mathbf{S}) - \mathbf{B}\|_F^2 = \sum_{j=1}^{N} \min_{\boldsymbol{\sigma}_j} \|M(\boldsymbol{\sigma}_j) - \mathbf{b}_j\|_2^2, \tag{16}$$

where $\|\cdot\|_F$ denotes the Frobenius norm and $\mathbf{M}(\mathbf{S}) = [M(\boldsymbol{\sigma}_1), \ldots, M(\boldsymbol{\sigma}_N)]$ contains the readings predicted by the model. In (16) the two-dimensional problem is brought to N independent one-dimensional problems. Therefore, each one-dimensional problem is solved independently from each others and the obtained solutions are placed side by side to obtain the two-dimensional reconstruction. Each nonlinear least-squares problem for a single column is solved by the Gauss–Newton method regularized by the TGSVD or by the Tikhonov approach, as well as by the TMNGN2 method, as explained in Section 3. For each $j = 1, \ldots, N$, we initialize the starting point $\boldsymbol{\sigma}_j^{(0)}$ with a vector whose components are randomly and uniformly distributed within the intervals $(0.48, 0.52)$, $(1.48, 1.52)$, and $(1.49, 1.51)$. We observe that this differs from the initial point chosen in previous papers, e.g., in [13,14], where the authors adopted a vector with all equal entries (e.g., $[0.5, \ldots, 0.5]^T$ or $[1.5, \ldots, 1.5]^T$). Our choice emphasizes, in

the numerical experiments, that the TMNGN2 method is not affected by a random starting point, as it happens instead in the classical regularization method if we do not use a vector with equal components.

For all iterative methods, the damping parameter α_k is determined by coupling the Armijo–Goldstein principle (4) to the positivity constraint $\boldsymbol{\sigma}_j^{(k)} \geq 0$. Moreover, for the TMNGN2 method, the second relaxation parameter β_k is determined by an automatic procedure based on the comparison between the residue obtained from TMNGN2 and the residual of Gauss–Newton at the same step; the algorithm to choose β_k is explained in detail in [38]. For all iterative methods, we adopt the following stopping criterion: fixed a tolerance $\tau > 0$, we iterate until the difference between two successive approximations is small enough

$$\|\boldsymbol{\sigma}_j^{(k)} - \boldsymbol{\sigma}_j^{(k-1)}\|_2 < \tau \|\boldsymbol{\sigma}_j^{(k)}\|_2,$$

or until a chosen maximum number of iterations $K_{\max}$ is reached. In our numerical tests, we set $\tau = 10^{-8}$ and $K_{\max} = 100$. An additional stopping rule is considered, in order to detect the unboundedness of the approximate solution for a particular value of the regularization parameter. The iteration is interrupted if the ratio between the norms of the kth approximate solution and the starting point $\boldsymbol{\sigma}_j^{(0)}$ is larger than a certain threshold, which in the numerical experiments of this paper is set to 10^8. This indicates that the solution is growing without bound and is therefore unlikely to converge to a meaningful result. This stopping rule is useful in the case where the regularization parameter is not well chosen and the computed solution is unbounded. By interrupting the iteration, the user can investigate the cause of the unboundedness and adjust the regularization parameter accordingly. Without this stopping rule, the iteration may continue indefinitely, leading to an overflow or to misleading results.

5 Numerical Experiments

This section is devoted to analyzing the behavior of different regularized solution methods for the inversion problem. In particular, we compare the results obtained by applying the TGSVD with the minimization of the Tikhonov functional and with the TMNGN2 method.

All the computations were carried out in Matlab version 9.10 (R2021a) on an Intel(R) Xeon(R) Gold 6136 server with 128 GB of RAM memory and 32 cores, running the Ubuntu/Linux operating system.

We consider synthetic data by generating two test models for the electrical conductivity. They are illustrated in the first picture of Fig. 2 and Fig. 4. To generate the synthetic data, we choose a particular configuration of the Geophex GEM-2 device, with both orientations of the coils, with inter-coil distance $\rho = 1.66$ m, six different operating frequencies $f = 775, 1175, 3925, 9825, 21725, 47025$ Hz, and two measuring heights $h = 0.8, 1.6$ m above the ground. Therefore, we have $m = 24$ data for each position $j = 1, \ldots, N$. Chosen $N = 50$ soundings along a 10 m path, the forward model generates the matrix $\widehat{\mathbf{B}}$ of dimension

$m \times N$ of the exact synthetic measurements. To simulate experimental errors, we add a noise vector to each column of $\widehat{\mathbf{B}}$

$$\mathbf{e}_j = \frac{\varepsilon \|\widehat{\mathbf{b}}_j\|_2}{\sqrt{m}} \mathbf{w}, \qquad j = 1, \ldots, N,$$

where $\mathbf{w}$ is a normally distributed random vector with zero mean and unitary variance and ε stands for the noise level. In our experiments, we set $\varepsilon = 10^{-3}$. We discretize the soil by $n = 60$ layers up to the depth of 3.5 m, each of which is of equal thickness. As a regularization matrix L we tested D_1 and D_2; see Eq. (8).

In Table 1 we report the relative restoration error (RRE) for each computed solution, defined by

$$\mathrm{RRE}(\mathbf{S}) = \frac{\|\mathbf{S} - \mathbf{S}_{\mathrm{exact}}\|_F}{\|\mathbf{S}_{\mathrm{exact}}\|_F},$$

where $\mathbf{S}_{\mathrm{exact}}$ is the exact solution.

Table 1. RRE obtained with different regularization techniques: the TGSVD, Tikhonov, and TMNGN2 methods. The algorithms are tested with different regularization matrices D_1 and D_2 and different starting points (random components uniformly distributed in the interval $(0.48, 0.52)$ and $(1.48, 1.52)$ for Example 1 and $(0.48, 0.52)$ and $(1.49, 1.51)$ for Example 2).

	Example 1				Example 2			
	$(0.48, 0.52)$		$(1.48, 1.52)$		$(0.48, 0.52)$		$(1.49, 1.51)$	
	D_1	D_2	D_1	D_2	D_1	D_2	D_1	D_2
TGSVD	0.1569	0.2303	0.1549	0.2304	0.1701	0.1851	0.1690	0.1799
Tikhonov	0.1576	0.2276	0.1578	0.2295	0.1653	0.1758	0.1661	0.1782
TMNGN2	0.1730	0.2152	0.1730	0.2152	0.1708	0.1782	0.1789	0.1780

From the errors shown in Table 1, it can be observed that for almost all algorithms, the errors obtained by regularizing the problem with the matrix D_1 are smaller, compared to the regularization matrix D_2.

Taking into consideration the matrix D_1 as a regularization matrix, we can observe that the RRE of the solutions obtained with the TGSVD and Tikhonov are smaller than the one obtained with the TMNGN2 method. In any case, however, in the right panel of Fig. 2 we can see some horizontal irregularities. These are caused by the lack of regularity of the solutions obtained with the TGSVD and the Tikhonov regularization. This lack of regularity can be shown by a graph of the electrical conductivity corresponding to only one column of $\mathbf{S}$. Fig. 3 depicts $\mathbf{S}(:, 33)$ on the left pane and $\mathbf{S}(:, 48)$ on the right for all iterative methods compared to the exact electrical conductivity in the same column. These irregularities do not occur in the solution computed with the TMNGN2 method.

By examining the RRE in Table 1, when $L = D_2$, the TMNGN2 recovers a better solution compared to the others, except in Example 2 and starting point in $(1.49, 1.51)$. Fig. 4 displays this case.

In both Fig. 2 and Fig. 4, we can notice some vertical artifacts or irregularities caused by the fact that we are solving N inverse problems independently of each other and we are chunking together their solutions. To avoid these irregular lines, one could think of reconstructing the 2D-solution as if it were an image. In this case, regularizers typically used in image restoration could be involved, which also induce horizontal regularization.

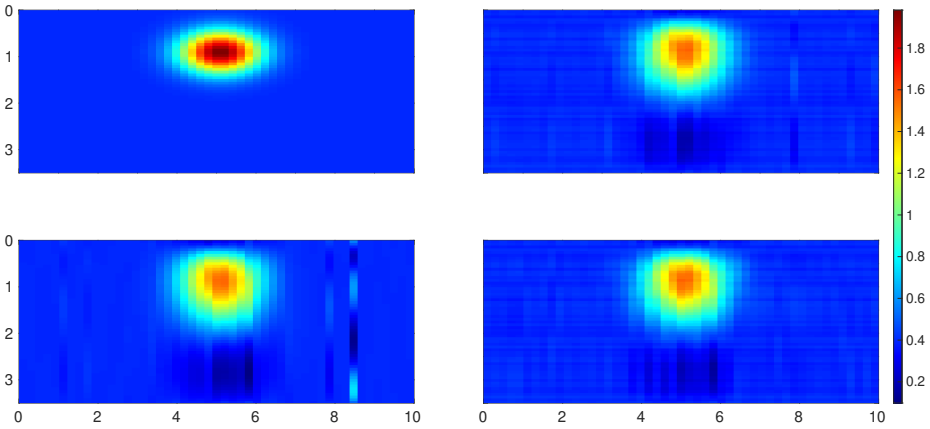

Fig. 2. Example 1. The exact solution (top-left) is compared to the solutions computed by TGSVD (top-right), by TMNGN2 (bottom-left), and by Tikhonov (bottom-right). The problem is regularized with matrix D_1. The initial point has random components uniformly distributed in the interval $(0.48, 0.52)$.

6 Conclusions and Future Developments

In this paper, we have tested the TMNGN2 method and we have compared it with TGSVD and Tikhonov regularization on an applied geophysics problem with the aim of reconstructing a 2D portion of the subsurface. We noticed that, compared to classical regularization methods, TMNGN2 does not suffer from an initial point with random entries.

The 2D reconstruction of a portion of the subsoil considered as an image and not arranging the 1D reconstructions side by side, will be a subject of study and research in the near future. This should allow to introduce "horizontal" regularization, by considering other regularization matrices that are usually used in image restoration, which would improve the reconstruction and avoid vertical irregularities, caused by a "side by side" reconstruction. Moreover, the applicability to 2D reconstructions is limited by the computational complexity of the

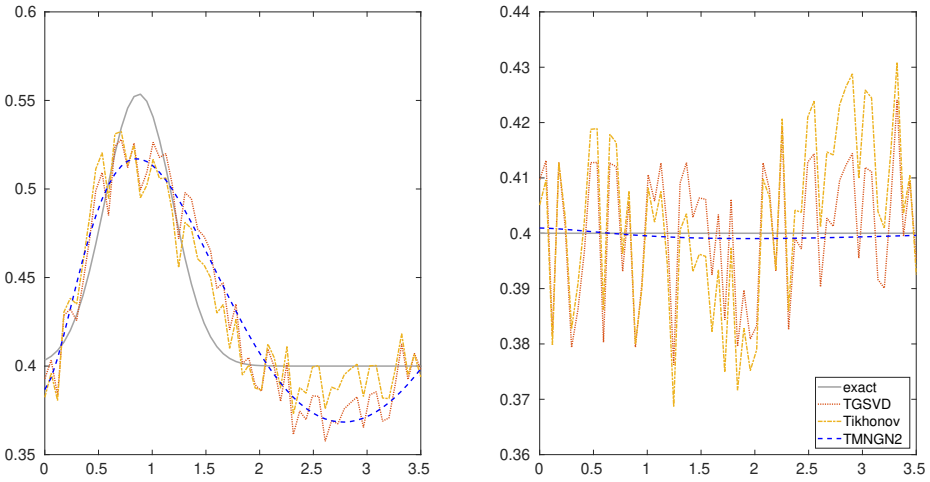

Fig. 3. Example 1. Electrical conductivity obtained from the 33rd (left) and 48th (right) dataset. The exact conductivity is compared to the solutions computed by TGSVD, by TMNGN2, and by Tikhonov. The problem is regularized with matrix D_1. The initial point has random components uniformly distributed in the interval $(0.48, 0.52)$.

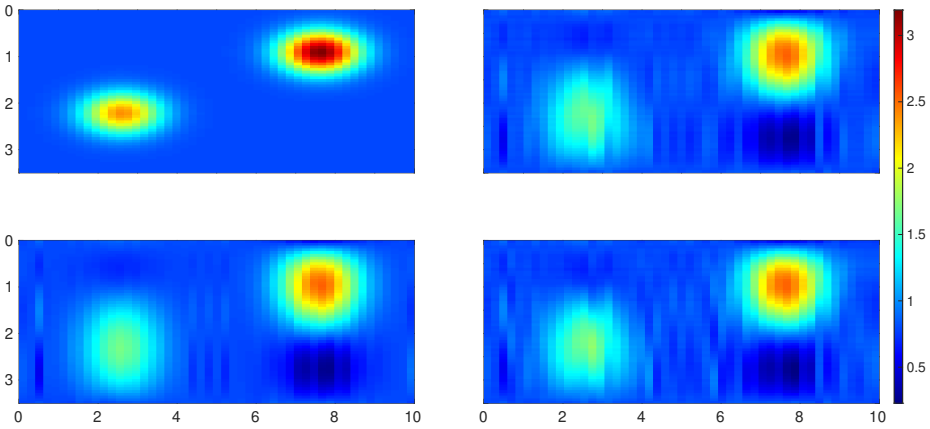

Fig. 4. Example 2. The exact solution (top-left) is compared to the solutions computed by TGSVD (top-right), by TMNGN2 (bottom-left), and by Tikhonov (bottom-right). The problem is regularized with matrix D_2. The initial point has random components uniformly distributed in the interval $(1.49, 1.51)$.

SVD. As done for instance in [2], the SVD could be replaced by Krylov subspace regularization methods.

Acknowledgements The author would like to thank Giuseppe Rodriguez for many precious discussions on the subject. The author is member of the GNCS group of INdAM and this research was partially funded by the INdAM-GNCS 2022 project "Metodi e modelli di regolarizzazione per problemi malposti di grandi dimensioni", by the INdAM-GNCS 2023 project "Tecniche numeriche per lo studio dei problemi inversi e l'analisi delle reti complesse", and by Fondazione di Sardegna, Progetto biennale bando 2021, "Computational Methods and Networks in Civil Engineering (COMANCHE)".

References

1. Armijo, L.: Minimization of functions having Lipschitz continuous first partial derivatives. Pac. J. Math. **16**(1), 1–3 (1966)
2. Bellavia, S., Donatelli, M., Riccietti, E.: An inexact non stationary Tikhonov procedure for large-scale nonlinear ill-posed problems. Inverse Probl. **36**(9), 095007 (2020). https://doi.org/10.1088/1361-6420/ab8f84
3. Björck, Å.: Numerical Methods for Least Squares Problems. SIAM, Philadelphia (1996). https://doi.org/10.1137/1.9781611971484
4. Boaga, J., Ghinassi, M., D'Alpaos, A., Deidda, G.P., Rodriguez, G., Cassiani, G.: Geophysical investigations unravel the vestiges of ancient meandering channels and their dynamics in tidal landscapes. Sci. Rep. **8**, 1708 (2018). https://doi.org/10.1038/s41598-018-20061-5
5. Borchers, B., Uram, T., Hendrickx, J.M.H.: Tikhonov regularization of electrical conductivity depth profiles in field soils. Soil Sci. Soc. Am. J. **61**(4), 1004–1009 (1997)
6. Buccini, A., Díaz de Alba, P.: A variational non-linear constrained model for the inversion of FDEM data. Inverse Probl. **38**(1), 014001 (2022). https://doi.org/10.1088/1361-6420/ac3c54
7. Buccini, A., Park, Y., Reichel, L.: Comparison of A-posteriori parameter choice rules for linear discrete ill-posed problems. J. Comput. Appl. Math. **373**, 112138 (2020). https://doi.org/10.1016/j.cam.2019.02.005
8. Buccini, A., Reichel, L.: Generalized cross validation for ℓ_p-ℓ_q minimization. Numer. Algorithms **88**, 1595–1616 (2021). https://doi.org/10.1007/s11075-021-01087-9
9. Deidda, G.P., Bonomi, E., Manzi, C.: Inversion of electrical conductivity data with Tikhonov regularization approach: some considerations. Annals for Geophysics **46**(3), 549–558 (2003). https://doi.org/10.4401/ag-3427
10. Deidda, G.P., Díaz de Alba, P., Fenu, C., Lovicu, G., Rodriguez, G.: FDEMtools: a MATLAB package for FDEM data inversion. Numer. Algorithms **84**, 1313–1327 (2020). https://doi.org/10.1007/s11075-019-00843-2
11. Deidda, G.P., Díaz de Alba, P., Pes, F., Rodriguez, G.: Forward Electromagnetic Induction Modelling in a Multilayered Half-Space: An Open-Source Software Tool. Remote Sens. **15**(7), 1772 (2023). https://doi.org/10.3390/rs15071772
12. Deidda, G.P., Díaz de Alba, P., Rodriguez, G.: Identifying the magnetic permeability in multi-frequency EM data inversion. Electron. Trans. Numer. Anal. **47**, 1–17 (2017)

13. Deidda, G.P., Díaz de Alba, P., Rodriguez, G., Vignoli, G.: Inversion of Multiconfiguration Complex EMI Data with Minimum Gradient Support Regularization: A Case Study. Math. Geosci. **52**(7), 945–970 (2020). https://doi.org/10.1007/s11004-020-09855-4
14. Deidda, G.P., Fenu, C., Rodriguez, G.: Regularized solution of a nonlinear problem in electromagnetic sounding. Inverse Probl. **30**(12), 125014 (2014). https://doi.org/10.1088/0266-5611/30/12/125014
15. Díaz de Alba, P., Fermo, L., van der Mee, C., Rodriguez, G.: Recovering the electrical conductivity of the soil via a linear integral model. J. Comput. Appl. Math. **352**, 132–145 (2019). https://doi.org/10.1016/j.cam.2018.11.034
16. Díaz de Alba, P., Fermo, L., Pes, F., Rodriguez, G.: Minimal-norm RKHS solution of an integral model in geo-electromagnetism. In: 2021 21st International Conference on Computational Science and Its Applications (ICCSA). pp. 21–28. Cagliari, Italy (Sep 2021). https://doi.org/10.1109/ICCSA54496.2021.00014
17. Díaz de Alba, P., Fermo, L., Pes, F., Rodriguez, G.: Regularized minimal-norm solution of an overdetermined system of first kind integral equations. Numer. Algorithms **92**, 471–502 (2023). https://doi.org/10.1007/s11075-022-01282-2
18. Dragonetti, G., Comegna, A., Ajeel, A., Deidda, G.P., Lamaddalena, N., Rodriguez, G., Vignoli, G., Coppola, A.: Calibrating electromagnetic induction conductivities with time-domain reflectometry measurements. Hydrol. Earth Syst. Sci. **22**, 1509–1523 (2018). https://doi.org/10.5194/hess-22-1509-2018
19. Engl, H.W., Hanke, M., Neubauer, A.: Regularization of Inverse Problems. Kluwer, Dordrecht (1996)
20. Eriksson, J., Wedin, P.A., Gullikson, M.E., Söderkvist, I.: Regularization methods for uniformly rank-deficient nonlinear least-squares problems. J. Optim. Theory Appl. **127**, 1–26 (2005). https://doi.org/10.1007/s10957-005-6389-0
21. Fenu, C., Reichel, L., Rodriguez, G., Sadok, H.: GCV for Tikhonov regularization by partial SVD. BIT **57**, 1019–1039 (2017). https://doi.org/10.1007/s10543-017-0662-0
22. Goldstein, A.A.: Constructive Real Analysis. Harper and Row (1967)
23. Golub, G.H., Heath, M., Wahba, G.: Generalized cross-validation as a method for choosing a good ridge parameter. Technometrics **21**(2), 215–223 (1979). https://doi.org/10.2307/1268518
24. Golub, G.H., Van Loan, C.F.: Matrix Computations. The John Hopkins University Press, Baltimore, third edn. (1996)
25. Hadamard, J.: Lectures on Cauchy's Problem in Linear Partial Differential Equations. Yale University Press, New Haven (1923)
26. Hansen, P.C.: Analysis of discrete ill-posed problems by means of the L-curve. SIAM Rev. **34**(4), 561–580 (1992). https://doi.org/10.1137/1034115
27. Hansen, P.C.: Rank-Deficient and Discrete Ill-Posed Problems. SIAM, Philadelphia (1998). https://doi.org/10.1137/1.9780898719697
28. Hansen, P.C., Jensen, T.K., Rodriguez, G.: An adaptive pruning algorithm for the discrete L-curve criterion. J. Comput. Appl. Math. **198**(2), 483–492 (2007). https://doi.org/10.1016/j.cam.2005.09.026
29. Hansen, P.C., O'Leary, D.P.: The use of the L-curve in the regularization of discrete ill-posed problems. SIAM J. Sci. Comput. **14**(6), 1487–1503 (1993). https://doi.org/10.1137/0914086
30. Hansen, P.C., Pereyra, V., Scherer, G.: Least Squares Data Fitting with Applications. Johns Hopkins University Press, Baltimore (2012)

31. Hendrickx, J.M.H., Borchers, B., Corwin, D.L., Lesch, S.M., Hilgendorf, A.C., Schlue, J.: Inversion of soil conductivity profiles from electromagnetic induction measurements: theory and experimental verification. Soil Sci. Soc. Am. J. **66**(3), 673–685 (2002). https://doi.org/10.2136/sssaj2002.6730
32. Hochstenbach, M.E., Reichel, L., Rodriguez, G.: Regularization parameter determination for discrete ill-posed problems. J. Comput. Appl. Math. **273**, 132–149 (2015). https://doi.org/10.1016/j.cam.2014.06.004
33. McNeill, J.D.: Electromagnetic terrain conductivity measurement at low induction numbers. Technical Note TN-6 Geonics Limited (1980)
34. Morozov, V.A.: The choice of parameter when solving functional equations by regularization. Dokl. Akad. Nauk SSSR **175**(6), 1225–1228 (1962)
35. Ortega, J.M., Rheinboldt, W.C.: Iterative Solution of Nonlinear Equations in Several Variables. Academic Press, New York (1970). https://doi.org/10.1137/1.9780898719468
36. Park, Y., Reichel, L., Rodriguez, G., Yu, X.: Parameter determination for Tikhonov regularization problems in general form. J. Comput. Appl. Math. **343**, 12–25 (2018). https://doi.org/10.1016/j.cam.2018.04.049
37. Pes, F., Rodriguez, G.: The minimal-norm Gauss-Newton method and some of its regularized variants. Electron. Trans. Numer. Anal. **53**, 459–480 (2020). https://doi.org/10.1553/etna_vol53s459
38. Pes, F., Rodriguez, G.: A doubly relaxed minimal-norm Gauss–Newton method for underdetermined nonlinear least-squares problems. Appl. Numer. Math. **171**, 233–248 (2022). https://doi.org/10.1016/j.apnum.2021.09.002
39. Reichel, L., Rodriguez, G.: Old and new parameter choice rules for discrete ill-posed problems. Numer. Algorithms **63**, 65–87 (2013). https://doi.org/10.1007/s11075-012-9612-8
40. Wait, J.R.: Geo-Electromagnetism. Academic Press, New York (1982)
41. Ward, S.H., Hohmann, G.W.: Electromagnetic Theory for Geophysical Applications. In: Electromagnetic Methods in Applied Geophysics: Voume 1, Theory, pp. 130–311. Society of Exploration Geophysicists (1988). https://doi.org/10.1190/1.9781560802631.ch4